

Investigation into the Influence of Feeding Parameters on the Formation of the Fed-Powder Layer in a Powder Bed Fusion (PBF) System

Ho-Jin Lee¹, Jae-Guk Song¹, and Dong-Gyu Ahn^{1#}

¹ Department of Mechanical Engineering, Chosun University, 309, Pilmun-daero, Dong-gu, Gwangju, 61452, South Korea
Corresponding Author / E-mail: smart@chosun.ac.kr, TEL: +82-62-230-7043, FAX: +82-62-230-7234

KEYWORDS: Powder bed fusion system, Additive manufacturing, Feeding parameters, Fed-powder layer, Proper feeding condition

Characteristics of the deposited layer in a powder bed fusion (PBF) system depend on the formation of the fed-powder layer. The objective of this paper is to investigate the influence of feeding parameters of the powder on the formation of the fed-powder layer in a PBF system. The effects of the gap between the feeding blade and the base plate, the volume of the powder and the supplied shape of the powder on the formation of the fed-powder layer and the defect mode of the powder bed were investigated via manual powder feeding experiments. From the results of the manual experiments, appropriate feeding conditions for achieving the desired formation of the fed-powder layer were estimated. The influence of the speed of the feeding blade and the supplied shape of powders on the formation of the fed-powder layer was examined through automatic powder feeding experiments. From the results of the automatic experiments, a practical speed of the feeding blade and an appropriate supplied shape of powders were determined.

Manuscript received: January 8, 2017 / Revised: January 17, 2017 / Accepted: January 31, 2017

NOMENCLATURE

φ = gap between feeding blade and base plate
 Ω = volume of the powder
 Δ = supplied shape of the powder
 ω = maximum width of the fed-powder layer
 ψ = width of the fed-powder layer in the centerline of the building platform
 ζ = maximum length of the fed-powder layer on the building platform
 η = filling ratio on the building platform
 λ_f = filled area by powders on the building platform
 λ_t = total area of the building platform
 $\varphi_{c,w}$ = critical gap from the viewpoint of the width of the fed-powder layer in the centerline of the building platform
 $\varphi_{c,l}$ = critical gap from the viewpoint of the maximum length of the fed-powder layer on the building platform
 φ_w = minimum gap without any defect
 κ = normalized volume ratio

t = deposition thickness of the powder
 d = diameter of the building platform
 V = speed of feeding blade
 $D_{p,max}$ = Maximum diameter of the powder

1. Introduction

In recent years, interest in additive manufacturing (AM) technology has been greatly increased due to its potential for easy fabrication of three-dimensional parts with arbitrary shapes using the layer-by-layer deposition.¹⁻⁴ Since the stereolithography process was developed by Charles Hull in 1984, various AM technologies have been introduced.^{1,4-6} The developed AM technologies can be classified into plastic and metal AM technologies according to the used material.^{1,5-7} The metal AM technologies can manufacture functional parts directly without additional processes, while the plastic AM technologies need a secondary process to fabricate functional parts.^{7,8} Sheet lamination, binder jetting, powder bed fusion (PBF), and direct energy deposition (DED) processes are

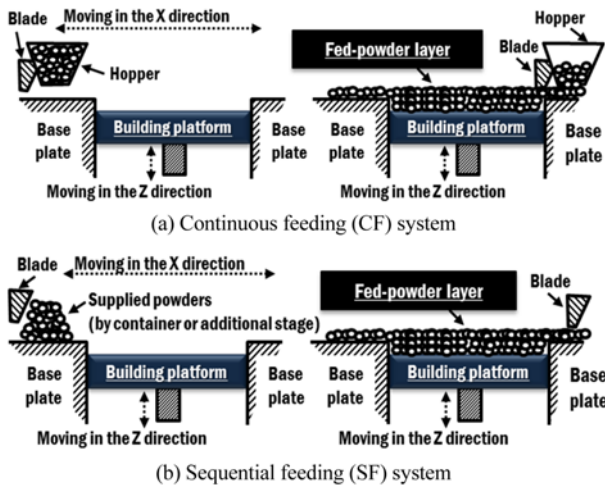


Fig. 1 Classification of the powder feeding system according to feeding methodology

Table 1 Feeding type of the commercialized PBF apparatus

Type of process	Type of PBS	Company	Model
Selective laser melting	CFD	SLM solution	SLM 500 HL ¹⁵
	SFD	Concept laser	M2 ¹⁶
Selective laser sintering	CFD	3D systems	Sinterstation HiQ ¹⁷
	SFD	3D systems	ProX SLS 500 ¹⁸
Direct metal laser sintering	CFD	3D systems	ProX 300 ¹⁹
	SFD	EOS	EOS M 280 ²⁰
Electron beam melting	SFD	ArcamAB	Q 20 ²¹

representative processes of the metal AM technology.⁷⁻¹⁰ Most of commercialized metal AM systems, including selective laser sintering (SLS), selective laser melting (SLM), direct metal laser sintering (DMLS), and electron beam melting (EBM) processes, use the PBF process as their fundamental working principle.^{7,9,10}

Metallic PBF processes include two sub-steps, such as powder feeding and deposition steps, to create metallic parts. In the powder feeding step, metallic powders are fed to the building platform to form a proper fed-powder layer.^{1,3,7-9} In order to create desired shapes in a layer, fed metallic powders are melted by high density energy sources, such as lasers and electron beams, and the melted powders are, subsequently, solidified. These sub-steps are repeated until a final layer is created. Finally, desired three-dimensional parts are fabricated.⁷⁻⁹

Characteristics of the deposited layer that occur in the deposition step, including shapes, thickness and width of the solidified bead, depend on the formation of the fed-powder layer. In order to obtain the deposited layer with the desired quality, the fed-powders should uniformly lie on the building platform without any defects. The deposition characteristics of the fed-powder layer are influenced by the feeder type and the feeding parameters. The commercial PBF system adopts two types of feeder including rollers and rakes with knife edges.¹¹⁻¹⁴

In the commercial PBF system with a rake type feeder, the feeding system of powders can be classified into a continuous feeding (CF) system and a sequential feeding (SF) system according to the feeding

methodology, as shown in Fig. 1 and Table 1.¹⁵⁻²¹ In the CF system, the feeder is attached to the hopper containing metallic powders, as shown in Fig. 1(a). The supply of powders through the hopper and the feeding of the supplied powders using the feeder are simultaneously carried out to create the fed-powder layer, as shown in Fig. 1(a). In the SF system, the feeder and the hopper are separated, as shown in Fig. 1(b). The powders are applied to the base plate through the hopper. Subsequently, the supplied powders are delivered to the building platform to form the fed-powder layer, as shown in Fig. 1(b).

Previous researchers have reported that representative feeding parameters of the commercial PBF system are the material of the feeder, the speed of the feeder, the material of the powder, the shape of the powder, the applied pressure to the powder, the volume of the powder, the geometry of the feeding system, etc..²²⁻²⁴ Van der Schueren and Kruth have researched the influence of the material of the powder on the packing density of the fed-powder layer for the case of SF systems with a blade type feeder. They have also investigated the effects of humidity on the flow rate of the powder for this system.²³ Kurzynowski et al. have investigated the influence of the grain size and the shape of the powder on the feeding characteristics.²⁴ Even though the formation of the fed-powder layer greatly affects the characteristics of the deposited layer, only a few research works has attempted to investigate the influence of feeding parameters on the formation of the fed-powder layer for the estimation of proper feeding conditions.

The objective of this paper is to investigate the influence of feeding parameters of the powder on the formation of the fed-powder layer in a PBF system. The effects of the gap between the feeding blade and the base plate, the volume of the powder, and the supplied shape of the powder on the formation of the fed-powder layer and the defect mode of the powder bed were investigated via manual powder feeding experiments. Feeding conditions appropriate to create the desired formation of the fed-powder layer were estimated. The influence of the speed of the feeding blade and the supplied shape of powders on the formation of the fed-powder layer was examined through automatic powder feeding experiments. A practical speed of the feeding blade and an appropriate supplied shape of powders were determined.

2. Experiments

2.1 Manual powder feeding experiments

In order to investigate the effects of feeding parameters on the formation and defect mode of the fed-powder layer, manual powder feeding experiments were performed. The gap between the feeding blade and the powder (ϕ), the volume of the powder (Ω) and the supplied shape of the powder (Δ) were chosen as feeding parameters of the manual powder feeding experiment, as shown in Fig. 2. Fig. 3 illustrates experimental set-up of the manual powder feeding experiment. The dimensions of the set-up for the manual powder feeding experiments were 240 mm \times 340 mm \times 104 mm, as shown in Fig. 3(a). The diameter of the building platform and the thickness of the deposited layer were set to 85 mm and 0.5 mm, respectively. The single blade with a knife edge was designed to feed the Stellite21 powders to the building platform, as shown in Fig. 3. The feeding width of the blade was 126 mm. The distance from the center of the supplied powder to

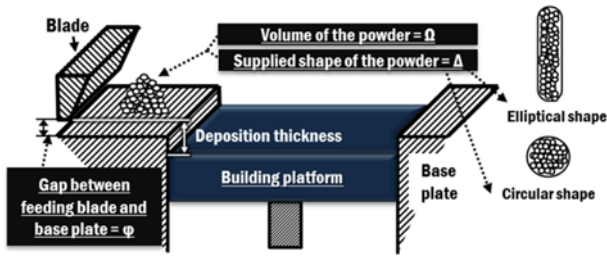


Fig. 2 Feeding parameters of manual powder feeding experiments

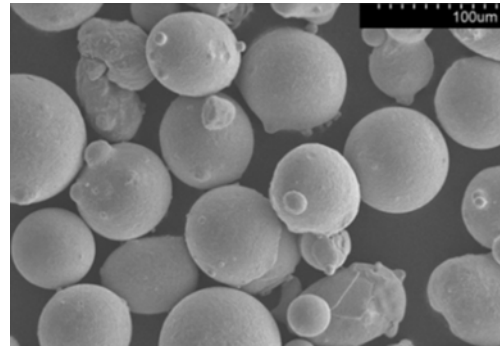


Fig. 4 Morphology of Stellite21 super-alloy powders

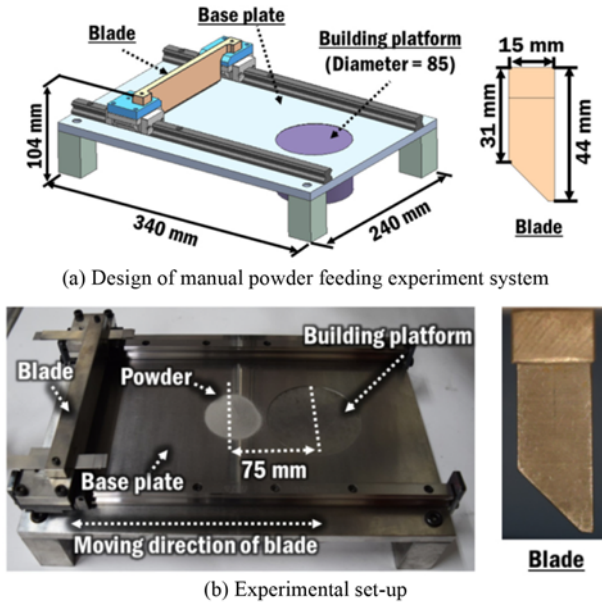


Fig. 3 Experimental set-up of manual powder feeding experiments

Table 2 Conditions of manual powder feeding experiments

ϕ (mm)	Ω (mL)	Δ
0.2-1.0	2.5-1.0	Elliptical and circular shapes

that of the building platform was set at 75 mm, as shown in Fig. 3. Table 2 shows conditions of the manual powder feeding experiments. The gap between the feeding blade and the base plate ranged from 0.2 to 1.0 mm. The volume of the powder lay in the range of 2.5-1.0 mL. Elliptical and circular shapes were chosen as the supplied shape of powders. Stellite21 super-alloy powders with a spherical shape were chosen as fed powders of the manual powder feeding experiment, as shown in Fig. 4. The diameter of the Stellite21 powders ranged from 45 to 150 μ m.

The maximum width of the fed-powder layer (ω), the width of the fed-powder layer at the centerline of the building platform (ψ), and the maximum length of the fed-powder layer on the building platform (ζ) were selected as measures to investigate the formation of the fed-powder layer quantitatively, as shown in Fig. 5. In addition, in order to examine the influence of the feeding parameters on filling characteristics of powders in the building platform, the filling ratio (h) was estimated using Eq. (1). Fig. 6 illustrates the definition of the filled area by powders on the building platform (l_f). The total area of the building platform (l_t)

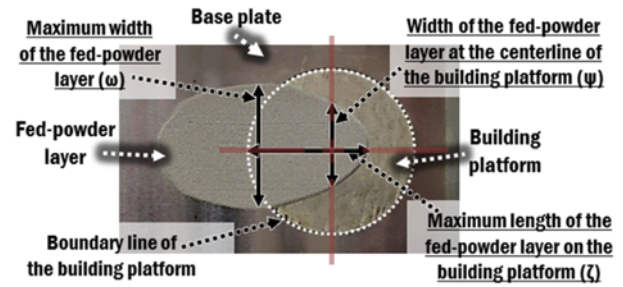


Fig. 5 Definition of the maximum width of the fed-powder layer (ω), the width of the fed-powder layer at the centerline of the building platform (ψ) and the maximum length of the fed-powder layer on the building platform (ζ)

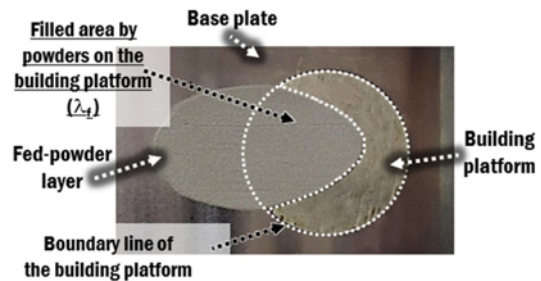


Fig. 6 Definition of the filled area by powders on the building platform (l_f)

was nearly 5,648 mm².

$$\eta (\%) = \frac{l_f}{l_t} \times 100 \tag{1}$$

2.2 Automatic powder feeding experiments

Automatic powder feeding experiments were carried out to investigate the influence of the speed of the feeding blade and the supplied shape of powders on the formation of the fed-powder layer. Fig. 7 shows the set-up of automatic powder feeding experiments. The diameter of the building platform of the deposited layer was set to 60 mm. The edge shape of the blade for the automatic feeding experiment was the same as that of the manual feeding experiment. The speed of

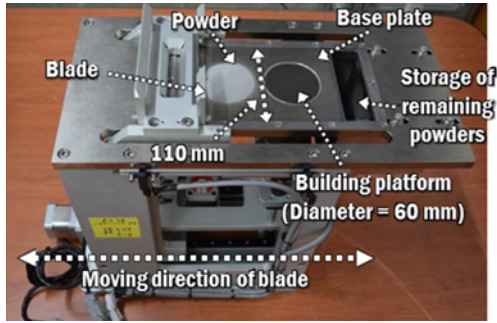


Fig. 7 Experimental set-up of automatic powder feeding experiments

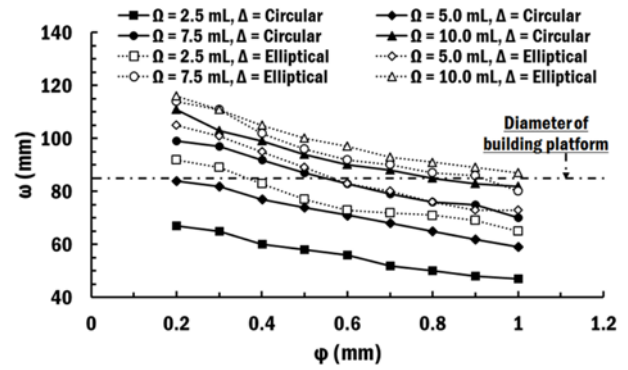
the feeding blade and the deposition thickness of the building platform were controlled by stepping motors and the PLC control system. The speed of the feeding blade (V) in the automatic powder feeding experiment ranges from 10 to 30 mm/s. The estimated proper feeding conditions, including the gap between the feeding blade and the powder, and the proper volume of the powder to be provided, from the manual powder feeding experiment were applied to the automatic powder feeding experiments.

3. Result and Discussion

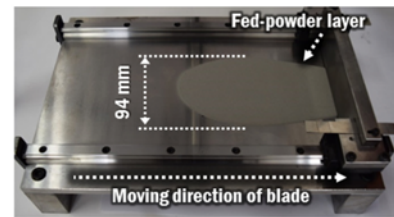
3.1 Formation of the Fed-powder Layer

The influence of feeding parameters on the maximum width of the fed-powder layer was investigated using results of manual powder feeding experiments, as shown in Fig. 8. The maximum width of the fed-powder layer decreased when the gap between the feeding blade and the base plate increased. This was due to the fact that the thickness of the fed-powder layer augmented when the gap increased. The maximum width of the fed-powder layer increased when the volume of the powder augmented. The maximum width of the fed-powder layer for the elliptical supplied shape of the powder was greater than that for the circular supplied shape of the powder by factors of nearly 1.1 to 1.4 times, as shown in Fig. 8. From this result, it was noted that the elliptical supplied shape was more effective than the circular supplied shape in terms of the formation of the fed-powder layer on the base plate. The ratio of increase in the maximum width of the fed-powder layer with the change in the supplied shape of powders from circular shape to elliptical shape decreased from 37% to 6% when the volume of the powder increased. From this result, it was concluded that the maximum width of the fed-powder layer was hardly influenced by the supplied shape of powders when the volume of the powder exceeded 10 mL. The maximum width of the fed-powder layer was smaller than the diameter of the building platform irrespective of the gap when the supplied shape of the powder and the range of the powder volume were circular and 2.5~5.0 mL, respectively, as shown in Figs. 8(a), (c) and (d).

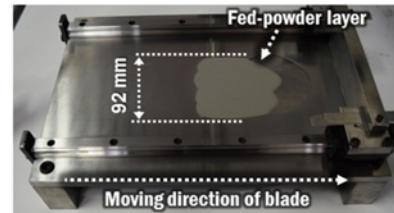
Fig. 9 shows the effects of feeding parameters on the width of the fed-powder layer at the centerline of the building platform. The fed-powder layer at the center line of the building platform of the circular supplied shape of powders were wider than those of the elliptical supplied shape of powders when the volume of the powder was 2.5 mL, as shown in Fig. 9. However, widths of the fed-powder layer for the



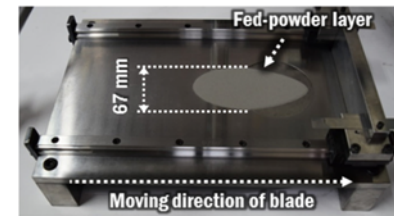
(a) Maximum widths for different feeding conditions



(b) $\Delta = \text{Circular}$, $\Omega = 10 \text{ mL}$ and $\phi = 0.5 \text{ mm}$



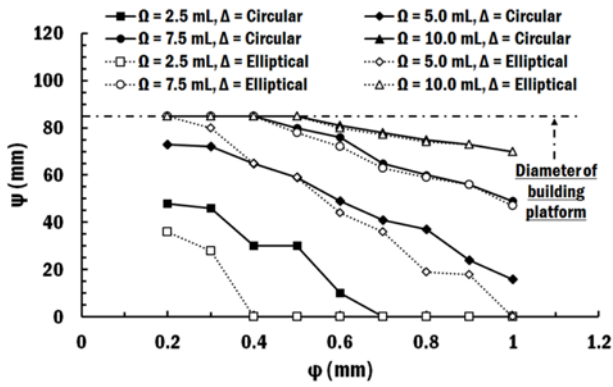
(c) $\Delta = \text{Elliptical}$, $\Omega = 2.5 \text{ mL}$ and $\phi = 0.2 \text{ mm}$



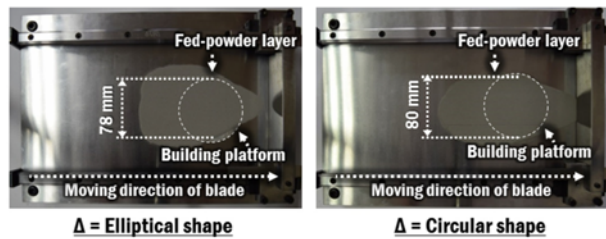
(d) $\Delta = \text{Circular}$, $\Omega = 2.5 \text{ mL}$ and $\phi = 0.2 \text{ mm}$

Fig. 8 Influence of feeding parameters on the maximum width of the fed-powder layer

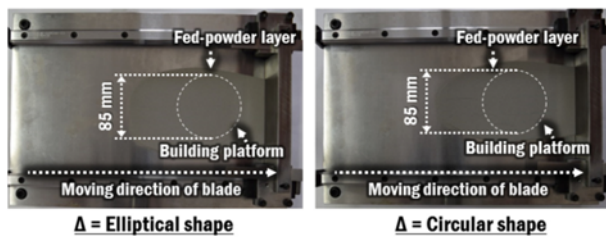
circular supplied shape of the powder were almost the same as those for the elliptical supplied shape of the powder when the volume of the powder was more than 7.5 mL, as shown in Figs. 9(a) and (b). The width of the fed-powder layer at the center line of the building platform was identical to the diameter of the building platform under several experimental conditions, as shown in Figs. 9(a) and (c). From this result, critical conditions needed to deposit powders fully on the building platform in the direction perpendicular to the feeding direction were estimated, as shown in Table 3. The minimum volume of the powder to fully deposit powders on the building platform in the direction perpendicular to the feeding direction was nearly 5.0 mL when the supplied shape of the powder was an elliptical shape, while that of the powder was nearly 7.5 mL when the supplied shape of the powder was a circular shape. This resulted from the fact that the initial width of the elliptical supplied shape of the powder was wider than that of the circular supplied shape of the powder. From those results, it was revealed that



(a) Width of the fed-powder layer for different feeding conditions



(b) $\Omega = 7.5$ mL and $\phi = 0.5$ mm



(c) $\Omega = 10$ mL and $\phi = 0.4$ mm

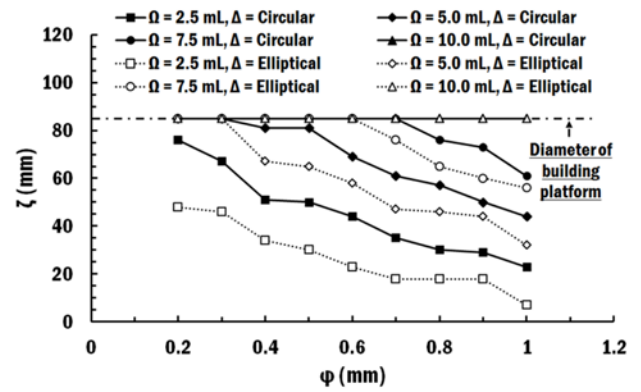
Fig. 9 Influence of feeding parameters on the width of the fed-powder layer at the centerline of the building platform

Table 3 Critical conditions to deposit powders fully on the building platform in the direction perpendicular to the feeding direction

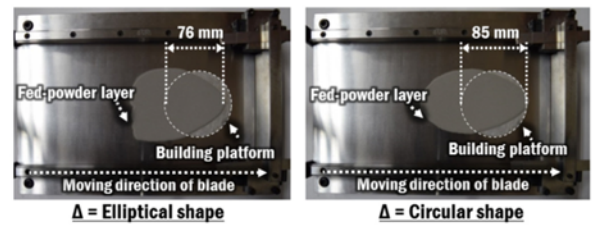
Δ	Ω (mL)	$\phi_{c,w}$ (mm)
Elliptical shape	5.0	0.2
	7.5	0.2-0.4
	10.0	0.2-0.5
Circular shape	7.5	0.2-0.4
	10.0	0.2-0.5

the elliptical supplied shape of the powder was superior to the circular supplied shape of the powder in terms of the deposition of the powder on the building platform in the direction perpendicular to the feeding direction.

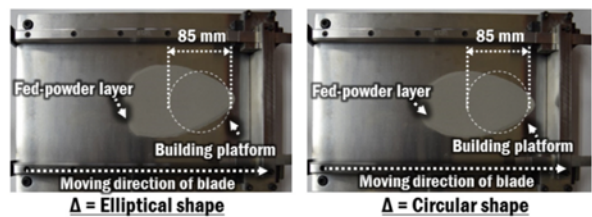
Fig. 10 shows the influence of feeding parameters on the maximum length of the fed-powder layer on the building platform. The maximum length of the fed powder on the building platform for the elliptical supplied shape of powders was shorter than those for the circular supplied shape of powders unlike the width of the fed-powder layer at the centerline of the building platform. From this result, it was noted that the elliptical supplied shape of the powder was inferior to the circular supplied shape of the powder from the viewpoint of the deposition of the powder on the building platform in the feeding



(a) Maximum length of the fed-powder layer for different feeding conditions



(b) $\Omega = 7.5$ mL and $\phi = 0.7$ mm



(c) $\Omega = 10.0$ mL and $\phi = 1.0$ mm

Fig. 10 Influence of feeding parameters on the maximum length of the fed-powder layer on the building platform

Table 4 Critical conditions to deposit powders fully on the building platform in the feeding direction

Δ	Ω (mL)	$\phi_{c,l}$ (mm)
Elliptical shape	5.0	0.2-0.3
	7.5	0.2-0.6
	10.0	0.2-1.0
Circular shape	5.0	0.2-0.3
	7.5	0.2-0.7
	10.0	0.2-1.0

direction. The maximum length of the fed-powder layer on the building platform was shorter than the diameter of the building platform irrespective of the supplied shape of the powder, and the gap between the feeding blade and the base plate when the volume of the powder is less than 2.5 mL. In contrast, the maximum length of the fed-powder layer on the building platform was identical to the diameter of the building platform regardless of the supplied shape of the powder and the gap, when the volume of powder was more than 10 mL, as shown in Fig. 10. The critical condition, for which the maximum length of the fed-powder layer was identical to the diameter of the building platform, began to appear when the volume of the powder was 5.0 mL, as shown in Fig. 10(a). The range of the desired gap between the feeding blade

Table 5 Conditions to examine the influence of feeding condition on the defect mode of the base plate and the fed-powder layer

Δ	Ω (mL)	$\varphi_{c,l}$ (mm)
Elliptical shape	7.5	0.2-0.4
	10.0	0.2-0.5
Circular shape	5.0	0.2
	7.5	0.2-0.4
	10.0	0.2-0.5

and the base plate, for which the maximum length of the fed-powder layer was the same as the diameter of the building platform, increased when the volume of the powder augmented. The range of the desired gap for the elliptical supplied shape of the powder was narrower than that for the circular supplied shape of the powder when the volume of the powder was 7.5 mL. Through the investigation of the influence of feeding parameters on the maximum length of the fed-powder layer on the building platform, critical feeding conditions were estimated from the viewpoint of the deposition of powder on the building platform in the feeding direction, as shown in Table 4.

3.2 Defect modes and practical feeding conditions

In order to estimate practical feeding conditions without any defects in the base plate and the fed-powder layer, the influence of feeding conditions on the defect mode of the base plate and the fed-powder layer was examined. The conditions, which satisfy the conditions in Tables 3 and 4 together, were applied to examine the defect mode in the base plate and the fed-powder layer, as shown in Table 5.

Through the investigation of the base plate and the fed-powder layer under the conditions in Table 5, two types of defect modes, including damage of the base plate and insufficient filling of powder on the building platform, were observed.

Several scratches were found in the base plate after finishing the manual feeding experiments for the condition of a gap of 0.2 mm, as shown in Fig. 11(a). This might be ascribed that scratches, which were induced by the trapping of powders between the base plate and the feeding blade, which accumulated on the base plate during the experiment under the condition of a gap of 0.2 mm. However, the scratches were not observed on the base plate irrespective of the supplied shape and the volume of the powder when the gap was more than 0.3 mm, as shown in Fig. 11(c). From these results, the minimum gap without any defect (φ_w) was determined to be 0.3 mm. Moreover, the relationship between the gap and the maximum diameter of the Stelle21 powder was estimated, as shown in Eq. (2).

$$\varphi_w = 2 \times D_{p,max} \quad (2)$$

The filling ratio was estimated for the conditions of Table 5 except for the gap of 0.2 mm, as shown in Fig. 12. The building platform was perfectly filled with the powder irrespective of the supplied shape of the powder, and the gap between the base plate and the feeding blade when the volume of the powder was 10.0 mL, as shown in Fig. 12. The filling ratio changed according to the gap between the base plate and the feeding blade when the volume of the powder was 7.5 mL, as shown in Figs. 12 and 13. The filling ratio was below 100% irrespective of the supplied shape of powders when the volume of the powder, and the gap between the base plate and the feeding blade were 7.5 mL and 0.4 mm,

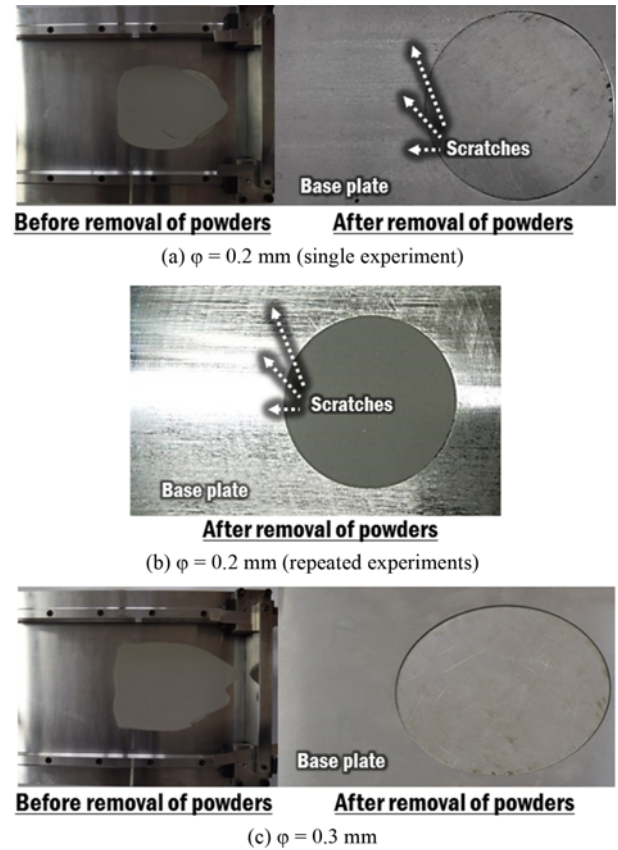


Fig. 11 Influence of the gap between the base plate and the feeding blade on the occurrence of scratches on the base plate (elliptical supplied shape of powders)

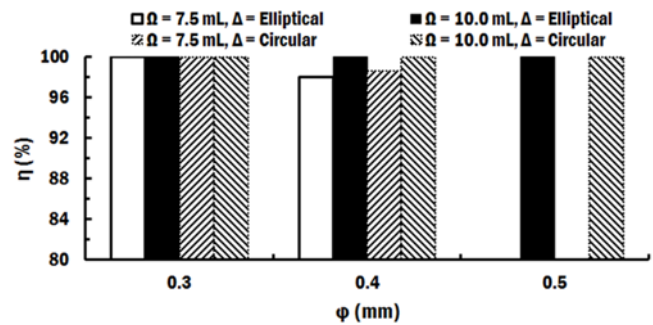


Fig. 12 Filling ratios for different feeding conditions

respectively, as shown in Figs. 12 and 13(a). However, the filling ratio was 100% irrespective of the supplied shape of the powder when the volume of the powder, and the gap between the base plate and the feeding blade were 7.5 mL and 0.3 mm, respectively, as shown in Figs. 12 and 13(b). The filling ratio of the circular supplied shape of the powder was slightly greater than that of the elliptical supplied shape of the powder when the volume of the powder, and the gap between the base plate and the feeding blade were 7.5 mL and 0.4 mm, respectively, as shown in Fig. 12.

From the results of the investigation of the defect mode and the filling ratio, the feeding map was estimated, as shown in Fig. 14.

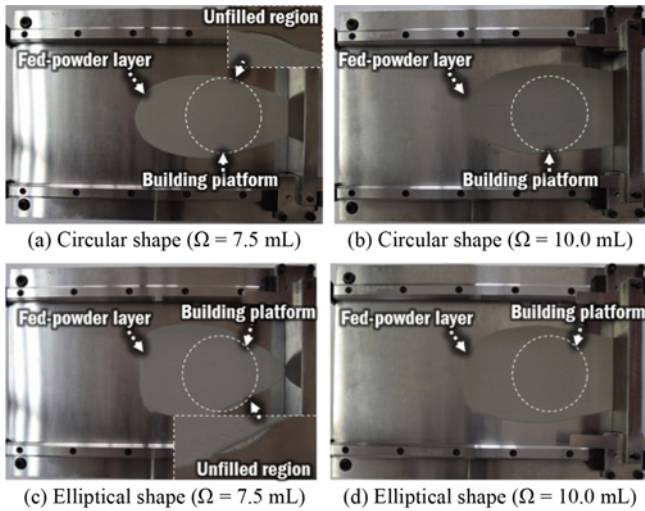


Fig. 13 Influence of the supplied shape and the volume of the powder on filling characteristics ($\phi = 0.4$ mm)

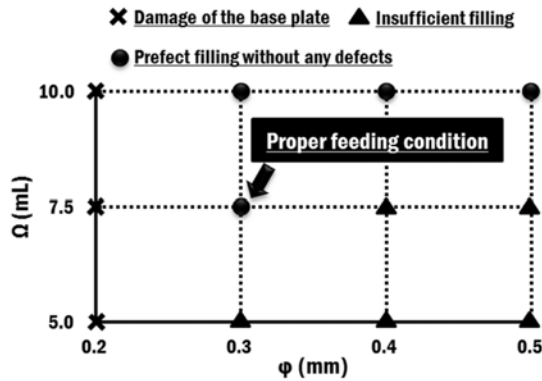


Fig. 14 Feeding map (circular and elliptical supplied shapes)

Table 6 Normalized volume ratios for perfect filling conditions ($\phi = 0.3$ mm)

Δ	Ω (mL)	κ
Elliptical and circular shapes	7.5	2.64
	10.0	3.53

Using the feeding map, the proper feeding condition was determined to be a gap of 0.3 mm and the powder volume of 7.5 mL, as shown in Fig. 14. In addition, normalized volume ratios for perfect filling conditions were predicted using Eq. (3). Table 6 shows the estimated normalized volume ratios for perfect filling conditions.

$$\kappa = \frac{4,000\Omega}{\pi d^2} \tag{3}$$

3.3 Speed of the feeding blade

The automatic feeding experiments were performed to determine a practical speed of the feeding blade. Using the results of the manual feeding experiment, the gap between feeding blade and base plate, and the normalized volume ratio were chosen as 0.3 mm and 2.64,

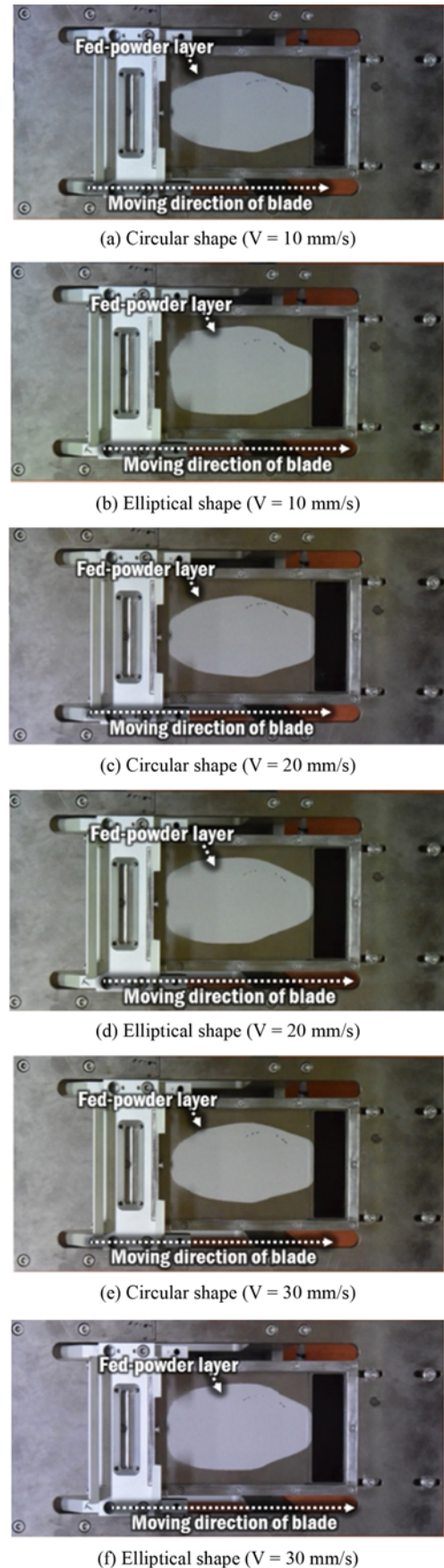


Fig. 15 Influence of the speed of feeding blade and the supplied shape of powders on the formation of the fed-powder layer ($\phi = 0.3$ mm and $\kappa = 2.64$)

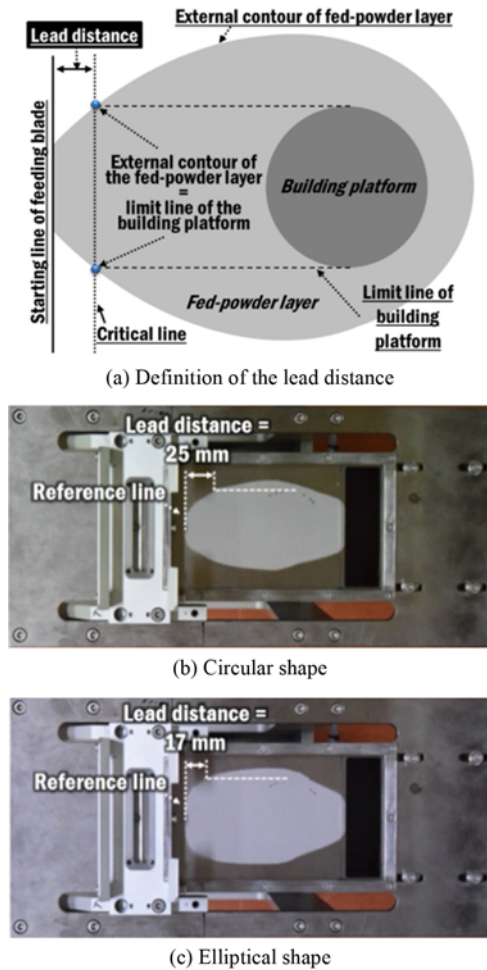


Fig. 16 Influence of the supplied shape of powders on the lead distance ($V = 30$ mm/s, $\phi = 0.3$ mm and $\kappa = 2.64$)

respectively. The volume of supplied powders in the automatic feeding experiments was predicted using Eq. (3). The estimated volume of the supplied powders was nearly 3.8 mL.

Fig. 15 shows results of the automatic feeding experiments. The building platform was perfectly filled by supplied powders irrespective of the speed of the feeding blade in the range of feeding speed used in the automatic feeding experiment. In addition, the filling pattern of the fed-powder layer was almost identical regardless of speed of the feeding blade. From those results, it was noted that the formation of the fed-powder layer on the building platform was hardly influenced by the speed of the feeding blade within the range of 10-30 mm/s. In addition, an appropriate speed of the feeding blade for the automatic powder feeding system was determined to be 30 mm/s.

The influence of the supplied shape of powders on the formation of the fed-powder layer under dynamic conditions was examined, as shown in Fig. 16. In an early stage of the powder feeding, the width of the fed-powder layer for the elliptical supplied shape of powders was wider than that for the circular supplied shape of powders. The lead distance was estimated to quantitatively investigate the effects of the shape of supplied powders on the fed-powder layer. Fig. 16(a) illustrates the definition of the lead distance. The lead distance for the elliptical supplied shape of shape.

4. Conclusions

In this paper, the influence of feeding parameters on the formation of the fed-powder layer in a PBF system was investigated via experiments.

The effects of the feeding parameters on the maximum width of the fed-powder layer, the width of the fed-powder layer at the centerline of the building platform, and the maximum length of the fed-powder layer on the building platform were examined via manual feeding experiments. The gap between the feeding blade and the base plate, the volume of powders, and the supplied shape of powders were chosen as the feeding parameters in the experiments. From the results of the examination, critical conditions to deposit powders fully on the building platform in both the direction perpendicular to the feeding direction and the feeding direction were estimated.

The influence of feeding conditions on the defect mode of the base plate and the fed-powder layer was investigated to estimate proper feeding conditions without any defects in the base plate and the fed-powder layer. Two types of defect modes, including damage of the base plate and insufficient filling of powders on the building plate, were observed. The damage of the base plate was mainly influenced by the gap between the feeding blade and the base plate. The relationship between the gap and the maximum diameter of the used powder was predicted to preserve the base plate from the damage. Perfect filling conditions were estimated to prevent insufficient filling of powders on the building platform. From the results of investigation of the defect mode and the filling ratio, a feeding map was created. Using the feeding map, an appropriate feeding condition has been determined to be a gap of 0.3 mm and the powder volume of 7.5 mL. In addition, normalized volume ratios for perfect filling conditions without any defects were estimated.

The effects of the speed of the feeding blade and the supplied shape of powders on the formation of the fed-powder layer under dynamic conditions were examined via automatic powder feeding experiments. From the results of the automatic experiments, a practical feeding speed was determined to be 30 mm/s. In addition, it was shown that the lead distance of the feeding blade in the PBF system and the amount of used powders could be considerably reduced when the supplied shape of powders was changed from a circular shape to an elliptical shape.

In future, additional experiments should be carried out to investigate the influence of shape, structure and dimension of the feeding blade on the formation of the fed-powder layer on the building plate.

ACKNOWLEDGEMENT

This work was supported by the Technology Innovation Program (10051336, Development of Core Technology of Rapid Manufacturing Process for Super-alloy with High Melting Temperature Using Electron Beam) funded by the Ministry of Trade, Industry & Energy, Korea.

REFERENCES

1. Bikas, H., Stavropoulos, P., and Chryssolouris, G., "Additive Manufacturing Methods and Modelling Approaches: A Critical

- Review,” *International Journal of Advanced Manufacturing Technology*, Vol. 83, Nos. 1-4, pp. 389-405, 2016.
2. Ko, H., Moon, S. K., and Hwang, J., “Design for Additive Manufacturing in Customized Products,” *Int. J. Precis. Eng. Manuf.*, Vol. 16, No. 11, pp. 2369-2375, 2015.
 3. Matsumoto, M., Yang, S., Martinsen, K., and Kainuma, Y., “Trends and Research Challenges in Remanufacturing,” *Int. J. Precis. Eng. Manuf.-Green Tech.*, Vol. 3, No. 1, pp. 129-142, 2016.
 4. Kang, H. S., Lee, J. Y., Choi, S. S., Kim, H., Park, J. H., et al., “Smart Manufacturing: Past Research, Present Findings, and Future Directions,” *Int. J. Precis. Eng. Manuf.-Green Tech.*, Vol. 3, No. 1, pp. 111-128, 2016.
 5. Ho, C. M. B., Ng, S. H., and Yoon, Y.-J., “A Review on 3D Printed Bioimplants,” *Int. J. Precis. Eng. Manuf.*, Vol. 16, No. 5, pp. 1035-1046, 2015.
 6. Gao, W., Zhang, Y., Ramanujan, D., Ramani, K., Chen, Y., et al., “The Status, Challenges, and Future of Additive Manufacturing in Engineering,” *Computer-Aided Design*, Vol. 69, pp. 65-89, 2015.
 7. Ahn, D.-G., “Direct Metal Additive Manufacturing Processes and their Sustainable Applications for Green Technology: A Review,” *Int. J. Precis. Eng. Manuf.-Green Tech.*, Vol. 3, No. 4, pp. 381-395, 2016.
 8. Cheah, C., Chua, C., Lee, C., Feng, C., and Totong, K., “Rapid Prototyping and Tooling Techniques: A Review of Applications for Rapid Investment Casting,” *International Journal of Advanced Manufacturing Technology*, Vol. 25, Nos. 3-4, pp. 308-320, 2005.
 9. Frazier, W.E., “Metal Additive Manufacturing: A Review,” *Journal of Materials Engineering and Performance*, Vol. 23, No. 6, pp. 1917-1928, 2014.
 10. Wohlers, T. T. and Caffrey, T., “Wohlers Report 2015: 3D Printing and Additive Manufacturing State of the Industry Annual Worldwide Progress Report,” Wohlers Associates, 2015.
 11. Beaman, J. J. and Deckard, C. R., “Selective Laser Sintering with Assisted Powder Handling,” US Patent, 4938816A, 1990.
 12. Deckard, C. R., Beaman, J. J., and Darrah, J. F., “Selective Laser Sintering with Layerwise Cross-Scanning,” WO Patent, 1992008567 A1, 1992.
 13. Colin, C., Bartout, J.-D., Shaker, E., Marchat, D., and Nimal, D., “Selective Laser Melting Process,” US Patent, 20160052162A1, 2016.
 14. Küsters, Y., Lupp, F., Rehme, O., and Schäfer, M., “Process for Selective Laser Melting and System for Carrying Out Said Process,” US Patent, 20140131921A1, 2014.
 15. SLM-SOLUTIONS, “Selective Laser Melting Machine SLM 500,” <https://slm-solutions.com/products/machines/selective-laser-melting-machine-slm-500> (Accessed 10 MAR 2017)
 16. CONCEPTLASER, “M2” <https://newsroom.concept-laser.de/videos.html> (Accessed 10 MAR 2017)
 17. Agile-Manufacturing Inc., “SINTERSTATION® HIQ™ SERIES SLS® SYSTEMS” <http://www.agile-manufacturing.com/files/products/sinterstation-hiq.pdf> (Accessed 10 MAR 2017)
 18. 3D SYSTEMS, “ProX SLS 500,” <https://www.3dsystems.com/3d-printers/prox-sls-500> (Accessed 7 MAR 2017)
 19. 3D SYSTEMS, “ProX DMP 300,” <https://www.3dsystems.com/3d-printers/prox-dmp-300> (Accessed 7 MAR 2017)
 20. e-Manufacturing Solutions, “EOSINT M 280,” https://www.eos.info/systems_solutions/metal/systems_equipment/eosint_m280 (Accessed 7 MAR 2017)
 21. Arcam AB, “Arcam Q20plus– for Production of Aerospace Components,” <http://www.arcam.com/technology/products/arcam-q20/> (Accessed 7 MAR 2017)
 22. Spears, T. G. and Gold, S. A., “In-Process Sensing in Selective Laser Melting (SLM) Additive Manufacturing,” *Integrating Materials and Manufacturing Innovation*, Vol. 5, No. 1, Article No. 2, 2016. (DOI: 10.1186/s40192-016-0045-4)
 23. Van der Schueren, B. and Kruth, J.-P., “Powder Deposition in Selective Metal Powder Sintering,” *Rapid Prototyping Journal*, Vol. 1, No. 3, pp. 23-31, 1995.
 24. Kurzynowski, T., Chlebus, E., Kuźnicka, B., and Reiner, J., “Parameters in Selective Laser Melting for Processing Metallic Powders,” *Proc. of SPIE*, Vol. 8239, Paper No. 823914, 2012. (DOI: 10.1117/12.907292)